Extended Abstracts of the 1995 International Conference on Solid State Devices and Materials, Osaka, 1995, pp. 142-144

Invited

Simulations of Crack Propagation and Fracture in Silica and Silicon Nitride Films on Parallel Computers

Priya VASHISHTA, Aiichiro NAKANO, and Rajiv K. KALIA

Concurrent Computing Laboratory for Materials Simulations
Department of Physics and Astronomy, and Department of Computer Science
Louisiana State University, Baton Rouge, LA 70803-4001, USA

Multiresolution molecular dynamics (MD) approach on parallel computers has been used to investigate the structural properties and mechanical failure in microporous silica and silicon nitride films. Critical behavior at fracture is analyzed in terms of pore percolation and kinetic roughening of fracture surfaces. Crack propagation in amorphous silicon nitride films is investigated, and a correlation between the speed of crack propagation and the morphology of fracture surfaces is observed.

KEY WORDS: Molecular Dynamics Method, Parallel Algorithms, Multiresolution Molecular Dynamics Approach, Crack Propagation, Fracture, Silica, Silicon Nitride, Ceramic Films

1. INTRODUCTION

Porous silica has been the focus of many investigations [1]. This environmentally safe material has numerous technological applications. Since these applications are due to the remarkable porous structure of the system, it is important to understand the size and spatial distributions of pores and the morphology of pore interfaces. Silicon nitride has been at the forefront of research for high-temperature, high-strength materials owing to its outstanding properties [2]. The combination of low thermal expansion and high strength makes silicon nitride one of the most thermal-shock-resistant materials currently available. Additionally, silicon nitride based films have found a number of applications in microelectronics technology. For these applications, the mechanism of fracture is one of the most important issues.

The morphology of fracture surfaces has drawn a great deal of attention in recent years [3-7]. It is now well-established that a fracture surface, z(x,y), is a self-affine object in that it remains invariant under the transformation, $(x, y, z) \rightarrow (ax, ay, a^{\zeta}z)$, where ζ is known as the roughness exponent. Bouchaud et al. carried out measurements of ζ for four aluminum alloys with different heat treatments and in each case they obtained $\zeta = 0.8$ [4]. Måløy et al. made measurements on six different brittle materials and found ζ to be 0.87 ± 0.07 [5]. This led them to conjecture that fracture surfaces of brittle and ductile materials had a "universal" roughness exponent, independent of material characteristics and the mode of fracture. Milman et al. questioned the validity of the "universality" of ζ, especially at microscopic length scales, by pointing out that their scanning tunneling microscopy data for MgO, Si, and Cu revealed the roughness exponent to be around 0.6 [6]. Measurements on tungsten and graphite also indicated a low value of ζ (≈ 0.4) [6]. However, recent MD simulations for such disparate systems as porous silica [7] and 2-d Lennard-Jonesium [8] found $\zeta \approx 0.8$.

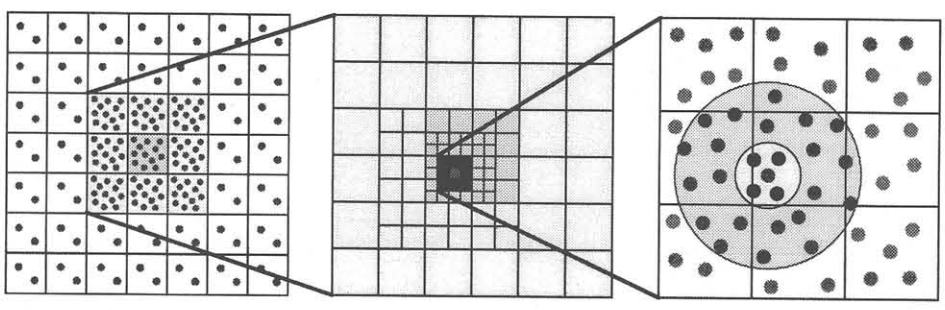

FIGURE 1: Schematic representation of the multiresolution algorithm. (a) Periodically repeated images of the original MD box. Replacing each well-separated image by a small number of particles with the same leading multipole expansions reduces the computation enormously while maintaining the necessary accuracy. (b) A hierarchy of cells in the fast multipole method. (c) The near-field forces on a particle are due to primary, secondary, and tertiary neighbor atoms.

2. MULTIRESOLUTION MD ALGORITHM

MD approach provides the phase-space trajectories of particles through the solution of Newton's equations. We are dealing with materials in which interatomic interactions are characterized by steric repulsion, Coulomb and charge-dipole interactions, and three-body covalent interactions. Highly efficient algorithms have been designed to compute these interactions on parallel machines [9]. The long-range Coulomb interaction is

calculated with a divide-and-conquer scheme, called the fast multipole method (FMM), which reduces the computational complexity from $O(N^2)$ to O(N). For short-ranged two- and three-body interactions, we have employed a multiple time-step (MTS) approach in which the force on a particle is subdivided into primary, secondary, and tertiary components (see Fig. 1). A significant reduction in computation is achieved by exploiting different time scales of these force components. For a 4.2 million particle silica glass, the execution time for a single MD time step is only 4.84 seconds on the 512-node Delta machine (see Fig. 2). The execution time scales linearly with the size of the system and the computation dominates the communication time.

3. FRACTURE OF SILICA GLASS

We have performed MD calculations on 1.12-million particle amorphous silica systems, investigating the growth of pores with a decrease in the density of the system [7]. As the normal-density glass is uniformly expanded, the pores begin to form when the density of the system is reduced to 1.8 g/cm^3. Further decrease in the density of the system causes an increase in the number of pores and also the pores coalesce to form larger entities (see Figure 3). There is a dramatic increase in the size of pores when the mass density is reduced to the critical value, ρ_c = 1.4 g/cm^3. At the critical density, some pores percolate through the entire system causing fracture.

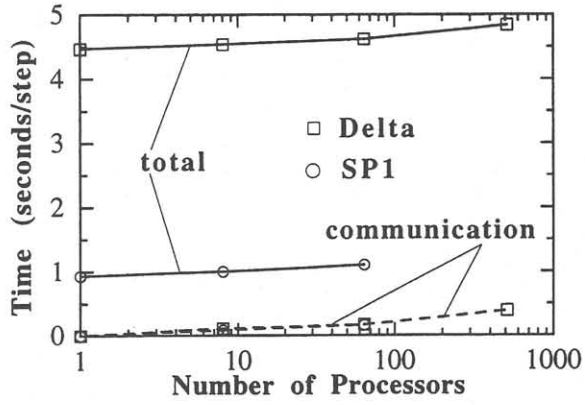

FIGURE 2: Execution time per step for multiresolution MD simulations of a-SiO_2 (solid curves) with 8,232p particles where p is the number of processors. Open squares and open circles are the results on the Delta and SP1, respectively. Dashed curves denote the communication overhead.

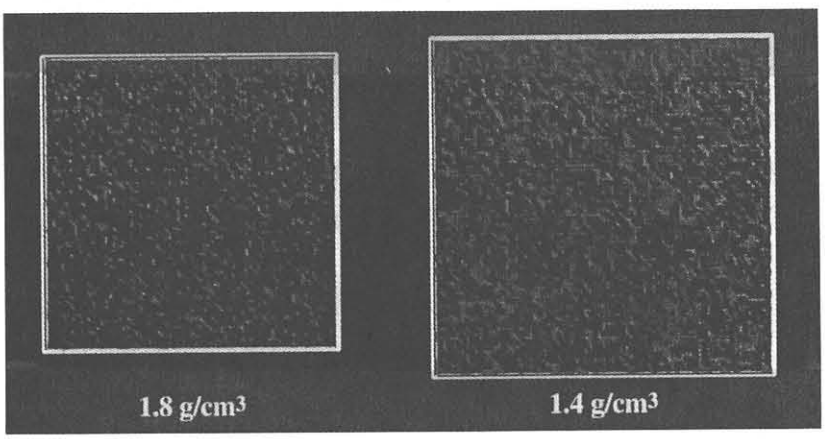

FIGURE 3: Snapshots of two-dimensional slices of MD configurations of silica (1.12 million particles) at densities 1.8 g/cm^3 and 1.4 g/cm^3.

The roughness of a fracture surface is calculated from the height-height correlation function, $G(\sigma)$, where σ is the horizontal distance. The MD results for $G(\sigma)$ are well-described by the relation, $G(\sigma) \sim \sigma^{\zeta}$ with $\zeta = 0.87 \pm 0.02$ for $\sigma < 10$ nm (see Fig. 4). The MD results for the roughness exponent agree with experimental measurements, thus indicating that the universality may prevail even at length scales ≤ 10 nm.

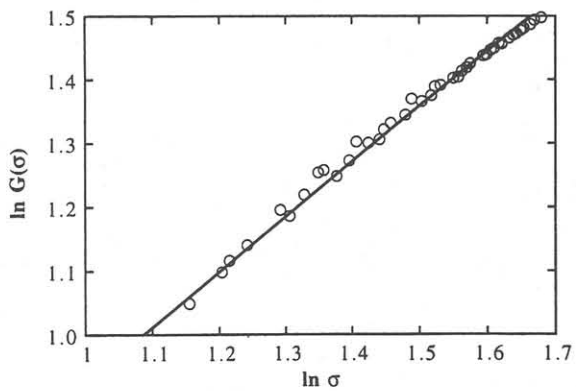

FIGURE 4: Height-height correlation function (open circles) versus the in-plane distance, σ, for the fracture surface of silica at 1.4 g/cm^3 The solid line is the best fit, $G(\sigma) \sim \sigma^{\zeta}$ with $\zeta = 0.87 \pm 0.02$ for $\sigma < 10$ nm

4. CRACK PROPAGATION IN a-Si_3N_4 FILMS

MD study of fracture in a-Si_3N_4 films involved systems with 100,352 atoms (typical dimensions of a film were 220Å × 220Å × 20Å), interacting via a combination

of two- and three-body potentials [10]. We first prepared well-thermalized bulk system by quenching the molten state and then periodic boundary conditions were removed and the systems were relaxed with MD and conjugate-gradient methods. These well-thermalized crystalline and amorphous Si_3N_4 films were subjected to uniaxial tensile loads by displacing atoms uniformly in the uppermost and lowermost layers (thickness ~ 5.5Å each) along the x direction. The strain was applied at a constant rate while maintaining the temperature at 300 K.

To investigate crack propagation, we insert a crack in an uniaxially stretched film (strain ~ 4 %) by removing particles within a region whose projection onto the xy plane is 4 Å × 50 Å, and we use a strain rate of 0.01 ps^{-1}. The crack plane is parallel to the yz plane, and the crack propagates along the y direction.

Figure 5 shows snapshots of the a-Si_3N_4 film projected onto the xy plane. Initially the crack propagates straight along the y direction, as shown in Fig. 5 (a), for the first 4.5 ps. At 7.9 ps, we observe the formation of voids in front of the crack tip, see Fig. 5 (b). These voids grow and form a secondary crack at t = 10.8 ps, see Fig. 5 (c). Eventually the secondary crack and the initial crack coalesce and the resulting crack surface is very rough, as evident from the snapshot in Fig. 5 (d) at t = 16.4 ps.

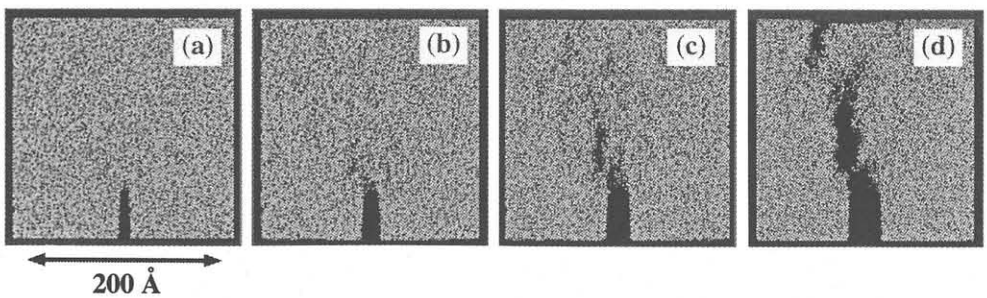

FIGURE 5: Snapshots of crack propagation in an a-Si_3N_4 film at time (a) 4.5 ps, (b) 7.9 ps, (c) 10.8 ps, and (d) 16.4 ps.

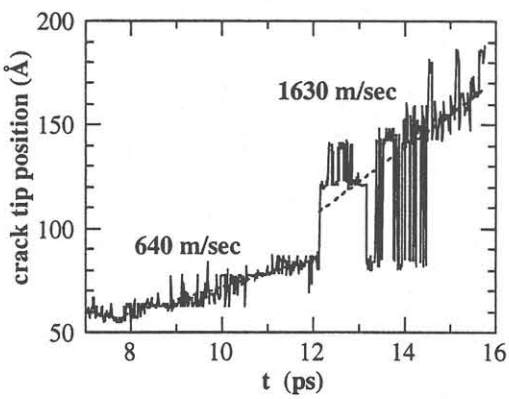

FIGURE 6: Crack tip position as a function of time (solid curves) in an a-Si_3N_4 film. Linear fits (dashed lines) before and after 12 ps give the average crack tip speed of 640 m/s (quasi-static) and 1630 m/s (rapid fracture), respectively.

To relate the morphology of the crack surface to the crack dynamics, we have examined the crack tip position as a function of time in the amorphous film. The crossover from quasi-static to rapid fracture is consistent with recent experiments and models of fracture [11-13]. For titanium aluminum alloys, Bouchaud and Navéos [11] observed a crossover of the roughness exponent from 0.45 to 0.84.

This work was supported by the U.S. Department of Energy, , National Science Foundation, , and Air Force Office of Scientific Research. and Louisiana LEQSF.

REFERENCES

1. J. Fricke, J. Non-Cryst. Solids **121** (1990) 188.
2. J. Mukerji, in *Chemistry of Advanced Materials*, ed. C. N. R. Rao, Blackwell (Oxford, 1993).
3. B. B. Mandelbrot, D. E. Passoja, and A. J. Paullay, Nature **308** (1984) 721.
4. E. Bouchaud, G. Lapasset, and J. Planès, Europhys. Lett. **13** (1990) 73.
5. K. J. Måløy, A. Hansen, E. L. Hinrichsen, and S. Roux, Phys. Rev. Lett. **68** (1992) 213; ibid. **71** (1993) 205.
6. V. Y. Milman, R. Blumenfeld, N. A. Stelmashenko, and R. C. Ball, Phys. Rev. Lett. **71** (1993) 204.
7. A. Nakano, R. K. Kalia, and P. Vashishta, Phys. Rev. Lett. **73** (1994) 2336.
8. F. F. Abraham, D. Brodbeck, R. A. Rafey, and W. E. Rudge, Phys. Rev. Lett. **73** (1994) 272.
9. R. K. Kalia, S. W. de Leeuw, A. Nakano, D. L. Greenwell, and P. Vashishta, Comput. Phys. Commun. **74** (1993) 316; A. Nakano, P. Vashishta, and R. K. Kalia, *ibid*. **77** (1993) 302; A. Nakano, R. K. Kalia, and P. Vashishta, *ibid*. **83** (1994) 197.
10. P. Vashishta, R. K. Kalia, and I. Ebbsjö: to be published in Phys. Rev. Letters (1995).
11. E. Bouchaud and S. Navéos, preprint.
12. J. P. Bouchard, E. Bouchard, G. Lapasset, and J. Planès, Phys. Rev. Lett. **71** (1993) 2240.
13. D. Etras and M. Karder, Phys. Rev. Lett. **69** (1992) 889.